

Observation of Dynamical Localization in Atomic Momentum Transfer: A New Testing Ground for Quantum Chaos

F. L. Moore, J. C. Robinson, C. Bharucha, P. E. Williams, and M. G. Raizen

Department of Physics, The University of Texas at Austin, Austin, Texas 78712

(Received 26 May 1994)

We report a direct observation of dynamical localization. This effect is a quantum suppression of diffusion in a system that is classically chaotic. Our experiment measures the momentum transferred from a modulated standing wave of a near-resonant laser to a sample of ultracold atoms and is a realization of a periodically driven rotor. The conceptual simplicity and experimental control over the time dependent Hamiltonian make this system an ideal testing ground for the predictions of quantum chaos.

PACS numbers: 05.45.+b, 32.80.Pj, 42.50.Vk, 72.15.Rn

The study of quantum systems that are chaotic in their classical limit has been the subject of intense research in recent years. Despite this fact, there remain many predictions which have not yet been verified experimentally due to the difficulty of realizing a dissipation-free model in which the time dependent Hamiltonian can be controlled. Perhaps the simplest version of such a model is the delta-kicked rotor, which has now become the paradigm for quantum chaos. The classical limit of this model gives rise to the standard map, which has been extensively studied in the context of Hamiltonian chaos. The quantum model predicts a suppression of classical diffusion due to dynamical localization, and has been related to a wide range of physical phenomena in which this effect is thought to occur [1–4]. One of the outstanding examples that has been studied experimentally is microwave ionization of Rydberg states of hydrogen [5,6].

The delta-kicked rotor is a particularly simple example of a larger class of one dimensional periodically driven rotors. One such model (which has a sinusoidal drive) was shown to exhibit localization and was directly related to the delta-kicked rotor for certain parameter regimes [7]. Although the drive potential is not turned on as a delta function, the evolution is composed of quasiperiodic resonant kicks which occur twice during each modulation period, with essentially free evolution in between.

In this Letter we report the first direct experimental realization of this periodically driven rotor and the observation of dynamical localization in this system. Our results are in good absolute agreement with predictions of Graham, Schlautmann, and Zoller [7], with no adjustable parameters. The conceptual simplicity of the experiment and the high degree of control over experimental parameters enables a broad range of experiments beyond the observation of dynamical localization, and should be a unique testing ground for many predictions in the field of quantum chaos.

The problem of atomic beam deflection in a modulated standing wave of light was first analyzed in Ref. [7]. The system consists of a two-level atom with a ground

state $|g\rangle$, an excited state $|e\rangle$, and an electric dipole allowed transition (dipole moment d) between these states with energy difference $\hbar\omega_0$. The atom interacts with a standing wave of near-resonant light (at frequency ω_L), where the standing wave position is modulated with an amplitude ΔL , at an angular frequency ω_m . For sufficiently large detuning $\delta_L = \omega_0 - \omega_L$ compared to the Rabi frequency, $\Omega/2 = dE_0/\hbar$, the dynamics are governed by stimulated two-photon scattering between ground states, with changes of momentum in units of $2\hbar k_L$. Classically, the atom behaves like a dipole in a conservative one dimensional periodic potential. The Hamiltonian in this limit is given by

$$H = p_x^2/2M - (\hbar\Omega_{\text{eff}}/8) \cos[2k_L(x - \Delta L \sin \omega_m t)],$$

where $\Omega_{\text{eff}} = \Omega^2/\delta_L$ is the effective Rabi frequency and k_L is the wave number. This Hamiltonian describes a periodically driven rotor and can be written in scaled dimensionless units as $H = p^2/2 - k \cos(\phi - \lambda \sin t)$. Here $k = \omega_r \Omega_{\text{eff}}/\omega_m^2$, where $\omega_r = \hbar k_L^2/2M$ is the recoil frequency, and $\lambda = 2k_L \Delta L$. The substitutions $t' = \omega_m t$, $\phi' = 2k_L x$, $p' = (2k_L/M\omega_m)p_x$, and $H' = (4k_L^2/M\omega_m^2)H$ have been made, and the primes were then dropped. In the quantized model, ϕ and p are the conjugate variables with a commutation relation $[p, \phi] = -i\hbar$, where $\hbar = 8\omega_r/\omega_m$ is the scaled Planck constant. The classical dynamics of this Hamiltonian are dominated by resonant kicks which occur when the atomic velocity matches the velocity of the modulated standing wave. This occurs twice during each modulation period and can lead to chaotic diffusion in phase space. When the atomic velocity exceeds the maximum velocity of the standing wave, which is proportional to λ , the resonant kicks turn off. Therefore this model, unlike the delta-kicked rotor, has a resonant kick boundary in phase space which scales linearly with λ . In the large chaotic domain, the quantum evolution of this time dependent Hamiltonian is governed by Floquet states which are expected to be exponentially localized in momentum space with a spread inversely proportional to λ [7]. The spread of atomic momentum in

time is then characterized by diffusive growth consistent with classical physics followed by saturation. For small values of λ , the saturation occurs near the resonant kick boundary, while as λ is increased beyond a critical value the saturation occurs at the quantum limit. This quantum limit has been approximated by the appropriate delta-kicked rotor with an initial condition of $p = 0$, and is shown in Fig. 1.

We now describe our experimental realization of this model. The original suggestion of Graham *et al.* [7] was to use angular deflection of an atomic beam passing through a modulated standing wave to measure momentum spread. A key technical point in our experiment was the realization that the momentum spread could be measured without the use of a beam by time resolved free expansion. The experiment can be summarized by

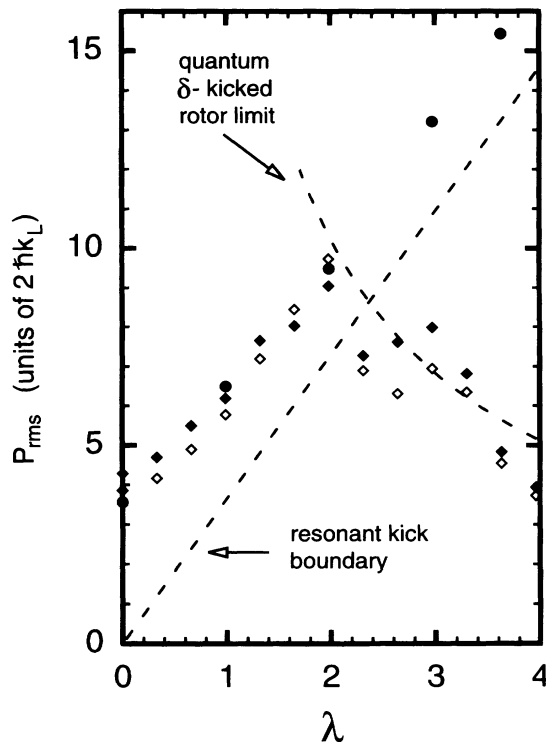


FIG. 1. rms momentum spread in units of $2\hbar k_L$ as a function of λ . The parameters for this curve are $\Omega_{\text{eff}}/2\pi = 22$ MHz (rms), $\delta_L/2\pi = 5.4$ GHz, $\omega_m/2\pi = 1.3$ MHz, $k = 0.34$ (rms), and $\tilde{k} = 0.16$. The straight and curved dashed lines denote the resonant kick boundary and the quantum δ -kicked rotor limit, respectively. The data are given for a duration of $10 \mu\text{s}$ (empty diamonds) and $20 \mu\text{s}$ (solid diamonds) and show that saturation has been reached. The solid circles are the result of a classical simulation and show agreement with the data up to a critical value of λ . Note that there are no adjustable parameters in this comparison between theory and experiment. The dominant experimental uncertainty is a 5% systematic in the value of k due to laser power calibration, and overlap of the standing wave with the atoms. This leads to a 10% uncertainty in the plotted quantum theory curve shown. Each data point has a 5% uncertainty in the rms momentum, with a 1% uncertainty in λ .

the following steps: We first trap and laser cool neutral atoms in a magneto-optic trap (MOT) [8]. This prepares the initial conditions for the experiment, by spatially confining a sample of ultracold atoms. The MOT is then turned off, and the modulated standing wave is turned on for a time t_m (typically $10 \mu\text{s}$), during which diffusive growth in momentum occurs along the direction of the modulated standing wave. This time is chosen to be somewhat longer than the calculated quantum saturation time, but short enough so that the probability of spontaneous emission is small (probabilities range between 10% and 20% in this work). After the standing wave is turned off, the atoms undergo free expansion in the dark for a time t_d (typically 5 ms). The final positions of the atoms are frozen in at that time by turning on the cooling beams in zero magnetic field to form an optical molasses [8], and the resulting atomic fluorescence is imaged on a charged couple device (CCD) camera. The initial size of the MOT is deconvolved, and the measurement of position is converted into a momentum spread using the time of flight.

The details of the experiment are now presented. Sodium atoms are trapped directly from the vapor in a magneto-optic cell trap [8]. The trap envelope consists of a quartz sphere of diameter 3" with nine 1.0" fused silica windows attached directly to the sphere. A sodium ampoule at room temperature is contained in a side-arm attached to the sphere. A conflat vacuum section is attached to the quartz sphere and the chamber is maintained at a base pressure of 5×10^{-10} Torr with a 20 l/s ion pump. A magnetic field gradient of 10 G/cm for trapping is provided by a pair of anti-Helmholtz coils. The residual field is nulled by 3-axis Helmholtz coils which surround the quartz envelope. A stabilized single-mode dye laser ($L1$) at 589 nm is pumped by an argon ion laser and is used for cooling, trapping, and detection of the sodium atoms. $L1$ is servo-locked to a saturated absorption peak in a sodium cell so that the trapping beams are maintained at a constant detuning of 20 MHz to the low frequency side of the $(3S_{1/2}, F = 2) \rightarrow (3P_{3/2}, F = 3)$ transition at 589 nm. The main beam from this laser passes through a resonant LiTaO_3 electro-optic phase modulator which is driven at 1.712 GHz. This imposes sidebands on the laser at the drive frequency, with a ratio of sideband to peak intensity of 20%, and prevents optical pumping of the sodium atoms into the $F = 1$ ground state. The beam then passes through an 80 MHz acousto-optic modulator (AOM) which is used both as a shutter and to stabilize the intensity fluctuations of $L1$ at the trap to approximately 1%. The laser is then coupled into a single-mode, polarization-preserving fiber which provides both spatial filtering and steering stability for the beams. The output of the fiber is collimated and split into three pairs of counterpropagating beams, which are polarized in a standard $\sigma_+ - \sigma_-$ configuration, and are aligned to overlap orthogonally in the center of the magnetic field gradient in order to establish the

MOT. Approximately 10^5 atoms are trapped within a diameter of 0.3 mm, and with a Gaussian momentum spread of $\sigma = 4.6\hbar k_L$. The region of beam overlap in the vacuum is approximately 8 cm^3 , which defines the usable volume for atom detection via the "freezing molasses." A second stabilized single-mode dye laser $L2$ is pumped by the same argon ion laser and is used to generate the modulated standing wave. Intensity fluctuations in this laser are actively stabilized with an AOM to approximately 1%. The lasers $L1$ and $L2$ are both mode matched into a marker cavity which has a free spectral range of 8.5 GHz and is scanned continuously. The marker cavity spacing and the reading of a wave meter (1 GHz resolution) then enable a measurement of the detuning of $L2$ from $L1$ to within 50 MHz. The output of $L2$ is collimated and split into two beams. Each beam passes through a separate 40 MHz AOM, and the first order diffracted beams are used. These modulators are used as shutters for $L2$, and are used to match the intensities of the two beams. One beam passes through an electro-optic phase modulator (EOM). This modulator is driven with an rf helical resonator at a frequency of $\omega_m/2\pi = 1.3 \text{ MHz}$. The phase modulation of one beam leads to a spatial modulation of the standing wave pattern, and the modulation index is λ . It can be adjusted in the range 0–15 by varying the amplitude of the rf drive, and is calibrated by optical heterodyne to an accuracy of better than 1%. The two beams are spatially filtered and the Gaussian beam profile is measured (waist of 1 mm at MOT). The two beams are aligned in a standing wave configuration which intersects the trapped atoms in the vacuum. The atomic fluorescence can be imaged on a video monitor camera and on a thermoelectrically cooled CCD. This enables a measurement of the initial MOT size and of the molasses size after free expansion. The entire sequence of the experiment as well as the data acquisition are computer controlled.

The experimental results are shown in Fig. 1, where rms momentum spread in units of $2\hbar k_L$ is given as a function of λ . Each data point was analyzed by the following procedure: The initial MOT size is deconvolved from the free expansion data, the spread in position is converted to momentum using the free expansion time, and a standard deviation is calculated for the resulting line shape. The data are plotted for the two cases of 10 and 20 μs duration of the modulated standing wave, and show that the momentum spread is near saturation for all values of λ . The dashed curved line is the theoretical prediction of a quantum delta-kicked rotor that was derived in [7] using our experimental parameters. The small variation of laser intensity across the atomic sample was included in the calculation of this curve which depends quadratically on intensity. It shows the $1/\lambda$ dependence in the localization length of the delta-kicked rotor derived (for large λ) from our Hamiltonian. A more accurate analysis predicts oscillations around

this curve [9]. This can be seen in our data and is supported by a numerical simulation of the quantum theory, following the same procedure outlined in Ref. [7]. These oscillations in localization length will be addressed in a separate publication in which the Floquet states for our Hamiltonian will be used to obtain a more precise comparison of theory to experiment. The solid circles in Fig. 1 are the result of a classical simulation, which accounts for the fast turn-on of the beams and the initial spread in momentum, and shows good agreement with the experiment for λ below a critical value. This classical simulation was run until saturation occurred and showed that classical diffusion actually saturated somewhat above the resonant kick boundary. For λ below 3.2, the classical spread is saturated by a time of 20 μs and therefore for regions between $\lambda = 2$ and $\lambda = 3.2$ our data clearly show dynamical localization. A unique feature of this experiment is that we obtain the actual atomic momentum distributions, and two representative samples are shown in Fig. 2. A crossover from the initial thermal distribution to one which is exponentially localized is clearly evident. Exponential distributions are characteristic of quantum localization within a classically chaotic phase space, as is the case in Fig. 2(b). Although this measurement is done on an ensemble of atoms, it is important to emphasize that the atoms are independent in this experiment and that the localization is a single atom quantum effect. The measured localized distribution can represent an *individual atomic wave packet* which was generated by the time dependent Hamiltonian. Generation of such "Floquet packets" constitutes a new direction in coherent atom optics using tailored time dependent potentials.

The conceptual simplicity of this system and our level of control over the time dependent Hamiltonian are unique features of this work, which should open up many new

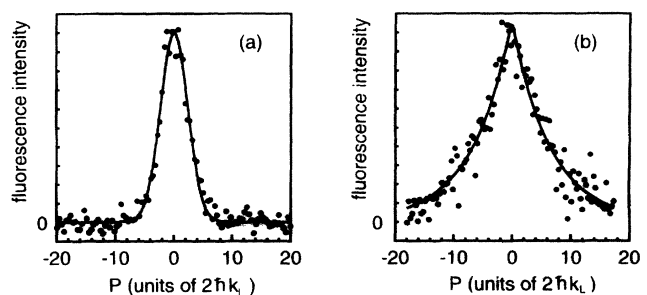


FIG. 2. Atomic momentum distributions. In (a) the distribution is shown for a MOT which is a typical initial condition for the measurements presented in Fig. 1. The least squares fit to the data is a Gaussian with $\sigma = 4.6\hbar k_L$ and represents an initial thermal distribution. In (b) the distribution is shown for $\lambda = 2.7$, and the parameters of Fig. 1. Also shown is the least squares fit by an exponential which is a characteristic of the Floquet distribution. A Poincaré surface of section for these parameters shows that the classical phase space is predominantly chaotic [16].

directions of research. Several of these directions are now outlined. (i) Beyond the observation of localization we can measure the diffusion in time [10], which should enable a direct measurement of the quantum “crossover time.” This can be achieved here by repeating the measurement for a range of interaction times of the standing wave with fixed values of the other parameters. The evolution of the cloud is then frozen in and measured with optical molasses at different stages of its growth. (ii) The effect of noise on dynamical localization has been investigated theoretically [11] and in microwave experiments [12]. In our experiment noise can be easily added with a second EOM or with the existing acousto-optic modulators. Delocalization is predicted for large enough noise drive, and this should be evident in the final spread as well as in the diffusive growth. (iii) The decoherence of a quantum system [13] can also be studied by turning on spontaneous emission. This can be accomplished either by tuning $L2$ closer to resonance, or by superimposing weak molasses beams with the modulated standing wave. (iv) The effects of a phase space boundary on dynamical localization are interesting to study since the dynamics are strongly influenced by the resonant kick boundary. Since localization occurs around initial conditions, we can observe boundary effects by preparing the atoms with a uniform nonzero initial velocity, or, equivalently, by imposing a drift velocity on the standing wave pattern. The boundary is reached when the drift velocity matches the maximum velocity of the modulation. (v) The role of dimensionality on localization has been studied extensively for the Anderson problem of electron conduction. It was shown that modulation of the delta-kicked rotor at incommensurate frequencies maps into the Anderson problem in two and three dimensions [14,15]. In the present system, the extra degrees of freedom can be attained by introducing additional modulation frequencies using electro-optic or acousto-optic modulators. (vi) The scaled Planck constant \hbar is an adjustable parameter in the experiment. In the present work it has a value of 0.16, which can be changed by varying the modulation frequency. By going to smaller values of that parameter, we can approach the classical limit which may open possible tests of quantum classical correspondence.

We would like to thank Martin Fischer and Michael Kaesbauer for technical assistance and Dr. Walter Buell for comments on the manuscript. We would also like to thank Professor Q. Niu, Professor L.E. Reichl, and Dr. Leo Hollberg for helpful discussions. This work was supported by the Office of Naval Research Young Investigator Program, the Welch Foundation, the A.P. Sloan Foundation, and the National Science Foundation Young Investigator Program.

-
- [1] R. V. Jensen, S. M. Susskind, and M. M. Sanders, *Phys. Rep.* **201**, 1 (1991).
 - [2] Chun-ho Iu, George R. Welch, Michael M. Kash, Daniel Kleppner, D. Delande, and J. C. Gay, *Phys. Rev. Lett.* **66**, 145 (1991).
 - [3] S. Fishman, D. R. Grepel, and R. E. Prange, *Phys. Rev. A* **29**, 1639 (1984).
 - [4] G. Casati, B. V. Chirikov, D. L. Shepelyansky, and I. Guarneri, *Phys. Rep.* **154**, 77 (1987).
 - [5] J. E. Bayfield and P. M. Koch, *Phys. Rev. Lett.* **33**, 258 (1974).
 - [6] P. M. Koch, in *Chaos and Quantum Chaos*, Proceedings of the Eighth South African School in Physics (Springer-Verlag, Berlin, 1993).
 - [7] R. Graham, M. Schlautmann, and P. Zoller, *Phys. Rev. A* **45**, R19 (1992).
 - [8] Laser cooling and trapping is reviewed by Steven Chu in *Science* **253**, 861 (1991).
 - [9] Q. Niu and R. Graham (private communication).
 - [10] B. V. Chirikov, *Chaos* **1**, 95 (1991).
 - [11] E. Ott, T. M. Antonson, Jr., and J. D. Hanson, *Phys. Rev. Lett.* **53**, 2187 (1984).
 - [12] R. Blümel, R. Graham, L. Sirko, U. Smilansky, H. Walther, and K. Yamada, *Phys. Rev. Lett.* **62**, 341 (1989).
 - [13] T. Dittrich and R. Graham, *Europhys. Lett.* **4**, 263 (1987); **7**, 287 (1988).
 - [14] D. L. Shepelyansky, *Physica (Amsterdam)* **8D**, 208 (1983).
 - [15] Giulio Casati, Italo Guarneri, and D. L. Shepelyansky, *Phys. Rev. Lett.* **62**, 345 (1989).
 - [16] Bala Sundaram (private communication).